Self-consistent electronic structure of FeAl

C. Koenig and M. A. Khan
Laboratoire de Magnétisme et de Structure Electronique des Solides, Laboratoire associé au Centre National de la Recherche Scientifique, No. 306, Université Louis Pasteur, 4 rue Blaise Pascal, F-67070 Strasbourg Cedex, France
(Received 8 September 1982; revised manuscript received 9 November 1982)

A self-consistent band structure of FeAl is obtained by the linearized muffin-tin orbitals method. The Fermi surface, positron localization, and the imaginary part $[\epsilon_2(\omega)]$ of the dielectric constant are calculated. A comparison is made with other theoretical and experimental results.

I. INTRODUCTION

The transition-metal aluminides (TAl) in general and FeAl in particular have been extensively studied for their soft-x-ray emission[1–3] (i.e., $TM_{2,3}$, TL_3, $TK\beta_{2,5}$, Al$L_{2,3}$, and Al$K\beta_x$) and absorption[2,4] (i.e., TL_3 and Al$L_{23,}$) properties. The single crystals of FeAl have been subjected to positron-annihilation[5] experiments to determine the localization of positrons. The positron-annihilation experiments on FeAl were also performed by Sob[6] and from these experiments the Compton profile was deduced. To understand these experimental data there are a few band-structure (BS) calculations of $B2$ ordered alloys.[6–11] Unfortunately, most of these are either non-self-consistent or only quasi-self-consistent. The self-consistent (SC) BS are obtained by the augmented-plane-wave[8–11] (APW) method, but to compute the physical properties, Eibler and Neckel[9] had to regenerate the BS in a hybridized nearly-free-electron tight-binding (H-NFE-TB) interpolation scheme.

The aim of the present work is to present a SC BS for FeAl and then to use these eigenvalues and eigenvectors to calculate other physical quantities such as the density of states, Fermi surface, positron localization, and the imaginary part of the dielectric constant. In the following we shall present a very short description of the linearized muffin-tin orbitals (LMTO) method (Sec. II) and then the results and discussion (Sec. III). Section IV will contain the conclusion.

II. METHOD

The LMTO method[12] is a standard technique these days for a SC BS calculation for ordered compounds.[13–15] A brief account of this method for CsCl structure has been already given by one of us.[16] Here we will just recall the main features.

The eigenenergies of the conduction states for ordered systems with many atoms per unit cell are obtained from the secular equation

$$|S^k_{\lambda'L',\lambda L}-P^\sigma_{\lambda l}(E)\delta_{\lambda'\lambda}\delta_{L'L}|=0\ , \tag{1}$$

where λ and σ are the site and spin indices, respectively. The index L is for the two quantum numbers l and m. We consider only the case when $l\leq 2$. According to this limitation we have $4s$, $3d$, and $4p$ for iron and $3s$, $3p$, and $3d$ for aluminum as the conduction states. $S^k_{\lambda'L',\lambda L}$ is the structure matrix.[12] We also have

$$P^\sigma_{\lambda l}=2(2l+1)\frac{D^\sigma_{\lambda l}(E)+l+1}{D^\sigma_{\lambda l}(E)-l}\ , \tag{2}$$

where

$$D^\sigma_{\lambda l}(E)=R_{\rm MT}\left[\frac{1}{\Phi^\sigma_{\lambda l}(E,r)}\frac{d}{dr}\Phi^\sigma_{\lambda l}(E,r)\right]_{r=R_{\rm MT}}\ , \tag{3}$$

i.e., it is a logarithmic derivative on the muffin-tin (MT) sphere ($r=R_{\rm MT}$) of the radial solution $\Phi^\sigma_{\lambda l}(E,r)$ of the Schrödinger equation in the potential V^σ_λ centered at a λ-type atom.

The simplest procedure to include the interstitial region is to approximate the MT sphere to an atomic sphere ($R_{\rm MT}=R_a$). This is the so-called atomic-sphere approximation[12] (ASA). For FeAl we have considered the same radii for iron and aluminum (i.e., $R=2.706$ a.u.). First, a SC canonical electronic band structure is obtained in which each type of atomic site forms a block and in each block there are independent subblocks of s, p, and d symmetries. The iteration was continued until we obtained the variation of the eigenenergies between two successive iterations less than 1 mRy. Once the SC canonical BS was obtained the hybridization between different atomic spheres and different symmetries was

switched on. The intersite charge transfer gives an ionic character to atomic sites. This additional Coulomb (Madelung) contribution to the potential was calculated by the method of Janak.[17] The exchange and correlation contributions to the potential are taken care of by the local-density-functional formalism.[18]

The hybridized SC BS was obtained after nine iterations when the overall eigenvalue differences between two successive iterations was less than 1 mRy. The total and local partial densities of states were calculated by the linear tetrahedron method.[19] For $\epsilon_2(\omega)$ we adapted the tetrahedron technique to make the summation over two states (i.e., occupied and unoccupied).

III. RESULTS AND DISCUSSION

A. Band structure and density of states

The SC BS of FeAl is presented in Fig. 1. The eigenvalues (in the limit of 1 Ry) at some high-symmetry points are given in Table I. With the use of this BS the total and local densities of states are calculated and presented in Fig. 2. We have also calculated the partial densities of states on each site and the main results are given in Table II. The $\frac{1}{48}$th of the Brillouin zone (BZ) of FeAl was divided into 1728 tetrahedrons (i.e., $\Gamma-X=12$ units in length). The densities of states are calculated with an energy interval of 2 mRy.

The present SC energy levels resemble other SC results.[8,10,11] As in these calculations, at high-symmetry point M below the Fermi level, we also obtain M_1 below M_5', whereas Sob[6] and Müller *et al.*[7] obtain M_5' below M_1. A comparison of present calculations with other SC and non-SC results is tentatively made and presented in Table III. One will notice that the total width of the occupied band $(E_F-E_{\Gamma_1})$ in our case is larger than those of Podloucky *et al.*[8] and Pechter *et al.*,[11] but on the

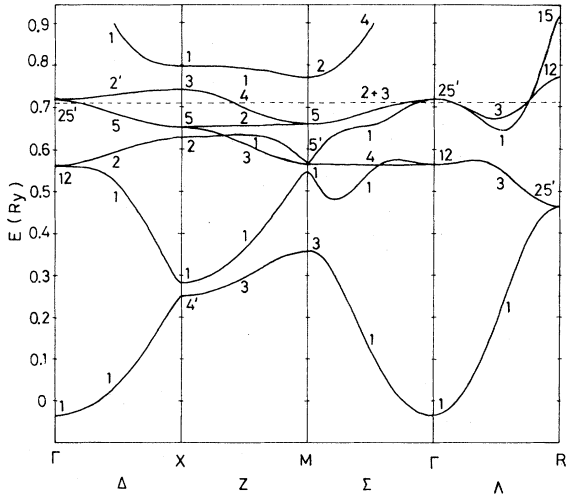

FIG. 1. SC energy bands in FeAl along some symmetry directions.

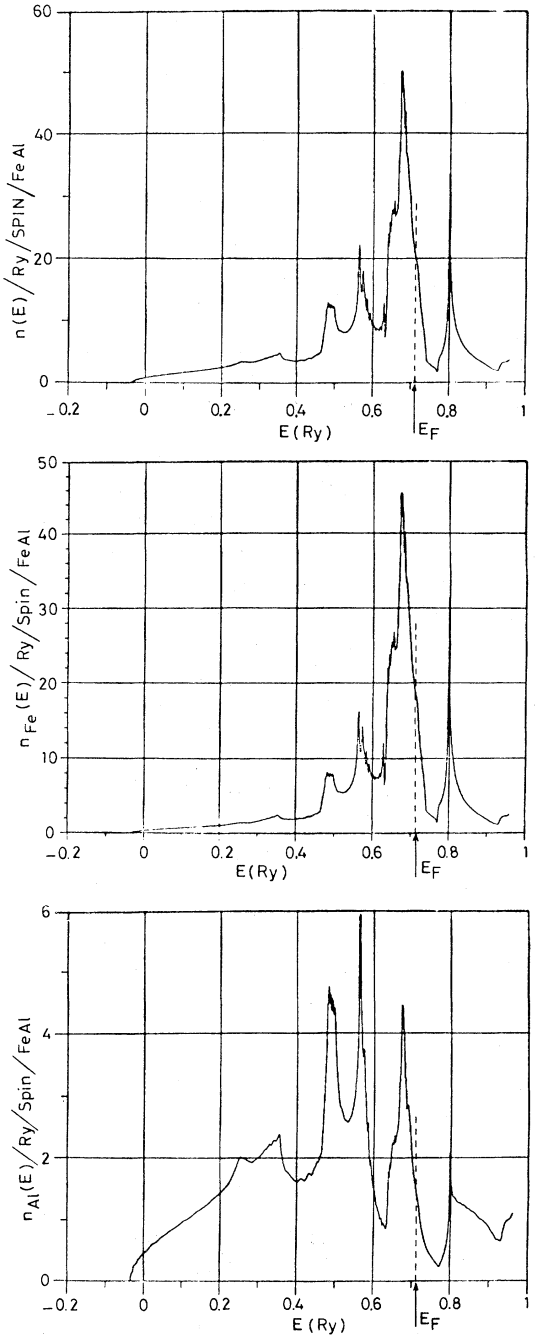

FIG. 2. (a) Total density of states of FeAl in units per FeRh molecules per Ry, (b) local density of states at an Fe site, and (c) local density of states at an Al site.

TABLE I. Present energy values (in rydbergs) at some high-symmetry points. The symmetry representations are enclosed in brackets.

Γ	−0.037 (1)	0.564 (12)	0.718 (25′)			
X	0.250 (4′)	0.281 (1)	0.628 (2)	0.653 (5)	0.724 (3)	0.798 (1)
M	0.357 (3)	0.547 (1)	0.565 (5′)	0.660 (5)	0.771 (2)	0.930 (1)
R	0.465 (25′)	0.773 (12)	0.917 (15)			

other hand, we have $E_{\Gamma'_{25}} - E_{\Gamma_{12}}$ smaller than theirs. The small differences in dispersion curves from one calculation to another may partially arise from the different approximations for exchange and correlation potential: Hedin-Lundqvist[18] in the present case and the Slater $X\alpha$ exchange with different values of α in the case of others.[8,10,11]

The overall features of the density of states are similar to those in Refs. 6, 7, and 9. From Table I and Fig. 2 it is evident that at the Fermi level the physical properties are mainly controlled by the "d" electrons of iron. The only specific-heat measurements[20] of FeAl gives the number of states at the Fermi level $[n(E_F)]$ as 31.3. Our value $n(E_F)=40.1$ is much greater than that observed. Eibler and Neckel[9] obtained $n(E_F)=32.05$, but later on they found that this value was in error due to the fact that it was not properly normalized in the unit cell.[21] The correct value[21] is $n(E_F)=42.9$ which is even higher than ours. Here we should mention the fact that the theoretical $n(E_F)$'s for FeAl are greater than the experimental one, whereas usually the measured $n(E_F)$'s are much bigger than the theoretical values[22] because the measured specific heat is already enhanced due to the electron-phonon interaction. From theoretical point of view, since the Fermi level falls in a sharp slope [Fig. 2(a)], it is possible to obtain an important change in $n(E_F)$ by shifting the E_F by a few mRy. In our scheme if we shift the $E_F=0.711$ Ry to $E'_F=0.720$ Ry, we do obtain $n(E'_F)=30$, but we have to content ourselves with 11.3 instead of 11.0 electrons in the occupied band. By shifting the Fermi level we also change the nature of the Fermi surface, particularly at the center of the BZ, which we shall discuss in the next section. Considering all these facts, may we suggest that further specific-heat measurements be made to check the only existing data.[20]

Table II shows a small charge transfer $\sim 0.27e$ from Al to Fe. The magnitude of the charge transfer is difficult to assess in APW calculations.[8–11] The measured charge transfer is $0.65e$ from Al to Fe.[7] Hence the trend of the theoretical charge transfer is in agreement with the experimental observation and also with the electronegativities[23] of 1.5 and 1.8 for Al and Fe, respectively.

TABLE II. Partial (n) densities of states and integrated number (N) of electrons at the Fermi level of different site λ (=Fe,Al) origin and symmetry l (=s,p,d) for a given spin σ. Densities of states are in units of per FeAl molecule per Ry.

	$n_s^\sigma(E_F)$	$n_p^\sigma(E_F)$	$n_d^\sigma(E_F)$ Γ'_{25}	Γ_{12}	$\sum_l n_l^\sigma(E_F)$	$\sum_{l,\sigma} n_l^\sigma(E_F)$
Fe	0.10	0.89	14.96	2.67	18.62	37.25
Al	0.017	0.49	0.92	0.008	1.43	2.87
	N_s^σ	N_p^σ	N_d^σ		$\sum_l N_l^\sigma$	$\sum_{l,\sigma} N_l^\sigma$
Fe	0.292	0.384	3.459		4.135	8.27
Al	0.455	0.701	0.210		1.366	2.73

TABLE III. Comparison between different calculations. Method used is indicated by "type," the exchange and correlation potential is denoted by "exch." Except for the results of Müller *et al.* (Ref. 7), the rest of the calculations presented in this table are SC.

Type Exch.	This work LMTO-ASA Hedin-Lundqvist	Refs. 8 and 11 APW X_α	Ref. 10 APW X_α	Ref. 7 H-NFE-TB
$E_F-E_{\Gamma_1}$	0.745	0.716		0.765
$E_F-E_{\Gamma'_{25}}$	−0.007	−0.018		
$E_F-E_{\Gamma_{12}}$	0.147	0.151		0.169
$E_{\Gamma'_{25}}-E_{\Gamma_{12}}$	0.154	0.169	0.171	
$E_{X_1}-E_{R'_{25}}$	0.333	0.312		~0.312

B. Fermi surface

While calculating the density of states by the tetrahedron method one looks for all the surfaces of a given constant energy in all the tetrahedrons. Out of 1728 tetrahedrons, 798 contained the Fermi surface of energy 0.711 Ry. Thus we could obtain a limited number of Fermi $\vec{k}$ vectors. In Fig. 3 we present the Fermi surface cuts in four symmetry planes (i.e., Γ-*X*-*M*, Γ-*X*-*R*, Γ-*M*-*R*, and *X*-*M*-*R*). The total area of the Fermi surface is 4.812 in units of $(2\pi/a)^2$, where $a=5.497$ a.u. Looking at the energy levels in Fig. 1, we notice that at Γ and *R* there are only three occupied states whereas at other high-symmetry points and directions there are always more than three which give the hole Fermi surfaces as Γ and *R*. The hole surface at *R* is much larger than that at Γ (Fig. 3). Pechter *et al.*[11] have also presented the intersection of the Fermi surface, but unfortunately, only in the Γ-*X*-*M* plane. They do point out the existence of the holes around Γ in the sheets corresponding to the fourth and fifth bands.

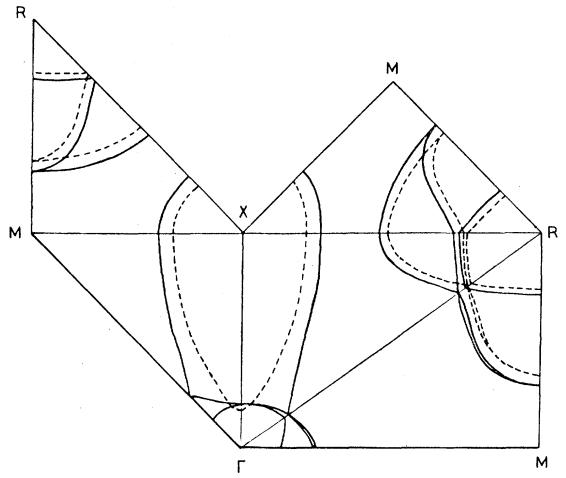

FIG. 3. Fermi-surface cross sections of FeAl in the symmetry planes Γ-*X*-*M*, Γ-*X*-*R*, Γ-*M*-*R*, and *X*-*M*-*R*. —— when $E_F=0.711$ Ry and − − − when $E_F=0.720$ Ry.

As mentioned earlier, the Fermi surface is very sensitive to E_F; we have also traced the Fermi-surface intersection (by dashed lines in Fig. 3), when $E_F=0.720$ Ry instead of 0.711 Ry. One will notice that by increasing E_F by 9 mRy makes the hole pockets around Γ disappear altogether. The hole pockets around *R* become smaller in size and the rest of the Fermi-surface intersections have been shifted *en bloc*. The total area of the Fermi surface becomes somewhat smaller [i.e., $3.335(2\pi/a)^2$].

To our knowledge there is no experimental data concerning the magnetothermal oscillations or de Hass—van Alphen effect in FeAl. But the different energy-level intersections with the Fermi level are indeed reflected in the dicontinuity in momentum-density curves observed by positron annihilation.[6] A direct measurement of the Fermi surface will certainly help to fix the Fermi level correctly.

C. Positron localization

One can estimate the localization of positrons at different sites in ordered or disordered compounds as a function of concentration by positron-annihilation experiments.[24] In FeAl we could calculate the probability P_λ^+ of finding the positron (+) on a site λ after obtaining the proper positron functions Ψ_λ^+. Since each atom of one type is surrounded by eight first neighbors of the other type, it is easy to construct the fundamental state of the positron in FeAl. At a given site λ the positron wave function Ψ_λ^+ is obtained by solving the Schrödinger equation

$$\left[-\frac{\Delta}{2}+V_\lambda^+(r)\right]\Psi_\lambda^+(r)=E^+\Psi_\lambda^+(r)\,, \tag{4}$$

where $V_\lambda^+(r)$ is the potential at the site λ experi-

enced by a positron. It is mainly the image at r axis of the one-electron Coulomb potential in FeAl. The functions $\Psi^+_{Fe}(r)$ and $\Psi^+_{Al}(r)$ are constrained to satisfy the continuity condition at the surface of the Wigner-Seitz (WS) spheres ($R_{WS}=2.706$ a.u.),

$$\Psi^+_{Al}(R_{WS})=\Psi^+_{Fe}(R_{WS})$$

and (5)

$$\left.\frac{d\Psi^+_{Al}(r)}{dr}\right|_{R_{WS}}=-\left.\frac{d\Psi^+_{Fe}(r)}{dr}\right|_{R_{WS}} .$$

The last condition determines the positron ground-state energy in the alloy. Once the $\Psi^+_\lambda(r)$ are properly determined, the probability P^+_λ of localization of the positron in the WS sphere centered on site λ is given by

$$P^+_\lambda=\frac{\int_{WS}|\Psi^+_\lambda(r)|^2 d^3r}{\int_{WS}|\Psi^+_{Fe}(r)|^2 d^3r+\int_{WS}|\Psi^+_{Al}(r)|^2 d^3r} . \quad (6)$$

We find that the two sites have the same probability: $P^+_{Fe}=0.502$ and $P^+_{Al}=0.498$. Since the wave function has a very flat slope at R_{WS}, the probabilities Π^+_λ of finding the positron in the inscribed spheres centered on each site are also nearly equal: $\Pi^+_{Fe}=0.318$, $\Pi^+_{Al}=0.316$, and

$$\Pi^+_{out}=1-(\Pi^+_{Fe}+\Pi^+_{Al})=0.365 .$$

This SC result confirms our previous calculations[25] using Herman-Skillman potentials on each site.

While calculating the positron charge distribution in FeAl Sob[6] found that it is proportional to iron and aluminum MT spheres, and hence there is no preference for a particular site. As for the experimental situation, positron localization has not been confirmed in pure FeAl, but on other binary alloys such as CdMg and AgAl (Ref. 24) no localization is observed. So our theoretical observation is consistent with other works.[6,24,26] If any localization in FeAl is ever observed experimentally, it will be due to the presence of vacancies or defects in the alloy.

D. Optical absorption

The optical absorption is proportional to the imaginary part of the dielectric function $\epsilon(q,\omega)$ with $q\simeq 0$ in the optical range. The imaginary part $\epsilon_2(\omega)$ of $\epsilon(\omega)$ arises from two distinct contributions: (i) Drude's term which is due to free charge carriers or free electrons, and then (ii) the interband transitions giving rise to structures in the optical-absorption curves,

$$\epsilon_2(\omega)=\epsilon^f_2(\omega)+\epsilon^b_2(\omega) , \quad (7)$$

where the free-electron part $\epsilon^f_2(\omega)$ is[27]

$$\epsilon^f_2(\omega)=\frac{4\pi N_f e^2}{m^*}\frac{\tau}{\omega(1+\omega^2\tau^2)} . \quad (8)$$

Here N_f is the number of free charge carriers per unit volume, and m^* is the optical effective mass which can be determined from the energy bands[28]; the relaxation time τ is determined from experimental measurements.

The interband part $\epsilon^b_2(\omega)$ (in a.u.) at 0 K is written as[29]

$$\epsilon^b_2(\omega)=\frac{1}{2\pi\omega^2}\sum_{\substack{n \\ \text{occupied}}}\sum_{\substack{n' \\ \text{unoccupied}}}\int_S |P_{nn'}(\vec{k})|^2\frac{dS_{\vec{k}}}{|\nabla_{\vec{k}}\omega_{nn'}(\vec{k})|} . \quad (9)$$

n and n' are occupied [$E_n(\vec{k})\le E_F$] and unoccupied [$E_{n'}(\vec{k})\ge E_F$] levels. $E_n(\vec{k})$ is the nth energy level at a given k vector and E_F is the Fermi level,

$$S=\{\vec{k}:\ E_{n'}(\vec{k})-E_n(\vec{k})=\omega_{nn'}(\vec{k})=\omega\} , \quad (10)$$

where ω is the photon frequency (or energy, since $\hbar=1$). $P_{nn'}(\vec{k})$ is the dipole matrix element. For numerical calculation we have adapted the tetrahedron method[13] to take into account the double sum over the occupied and empty states.

The Bloch functions are constructed as a sum of functions at different sites λ,

$$|nk\rangle=\sum_{l,m,\lambda}(i)^l C^{nk}_{lm\lambda}\Phi_l(r_\lambda)Y_{lm}(\hat{r}_\lambda) , \quad (11)$$

where the C's are the normalization factors, Φ_l is the radial part, and Y_{lm} is the angular part. Since the basis functions on each site in LMTO, vanish identically out of the atomic spheres, we obtain, therefore, the following expression at a given site:

$$\langle nk|\vec{P}|n'k\rangle=\sum_{l,m,l',m'} i^{(l'-l)}C^{*kn}_{lm}C^{kn'}_{l'm'}\langle\Phi_l(r)Y_{lm}(\hat{r})|\vec{P}|\Phi_{l'}(r)Y_{l'm'}(\hat{r})\rangle . \quad (12)$$

In the case of cubic crystals the dipole matrix will be isotropic for all the rectilinear directions, hence it suffices

to calculate only one of the three components. It is an easy matter to calculate $\langle nk \mid P_z \mid n'k' \rangle$ if we make use of the Wigner-Eckart theorem for the gradient formula.[30] Using

$$\frac{\partial}{\partial z} = \nabla_0 = \cos\theta \frac{\partial}{\partial r} - \frac{\sin\theta}{r} \frac{\partial}{\partial \theta} , \tag{13}$$

we obtain

$$\langle nk \mid \nabla_0 \mid n'k \rangle = \sum_{l,m} i^{(l\pm1)-l} C^{*kn}_{l,m} C^{kn'}_{l\pm1,m} (-1)^m \frac{\begin{pmatrix} l & 1 & l\pm1 \\ m & 0 & -m \end{pmatrix}}{\begin{pmatrix} l & 1 & l\pm1 \\ 0 & 0 & 0 \end{pmatrix}} \langle l,0 \mid \nabla_0 \mid l\pm1,0 \rangle , \tag{14}$$

where

$$\langle l,0 \mid \nabla_0 \mid l\pm1,0 \rangle = \langle \psi_l(r) Y_{l,0}(\hat{r}) \mid \nabla_0 \mid \psi_{l\pm1}(r) Y_{l\pm1,0}(\hat{r}) \rangle . \tag{15}$$

Thus, the dipole matrix finally contains only the radial integration. We have

$$\begin{pmatrix} j_1 & j_2 & j_3 \\ m_1 & m_2 & m_3 \end{pmatrix} ,$$

the so-called 3-j symbol of Wigner.[30] The other two components (i.e., $\langle nk \mid P_x \mid n'k \rangle$ and $\langle nk \mid P_y \mid n'k \rangle$) are easily obtained from the general expression[30]

$$\langle l',m' \mid \nabla_u \mid l,m \rangle = (-1)^{m'} \frac{\begin{pmatrix} l' & 1 & l \\ -m' & u & m \end{pmatrix}}{\begin{pmatrix} l' & 1 & l \\ 0 & 0 & 0 \end{pmatrix}} \langle l',0 \mid \nabla_0 \mid l,0 \rangle, \quad u = \pm 1 , \tag{16}$$

$$\nabla_1 = -\frac{1}{\sqrt{2}} \left(\frac{\partial}{\partial x} + i \frac{\partial}{\partial y} \right), \quad \nabla_{-1} = \frac{1}{\sqrt{2}} \left(\frac{\partial}{\partial x} - i \frac{\partial}{\partial y} \right) . \tag{17}$$

Thus we calculate the dipole matrix elements at the four corners of each tetrahedron; in between they are linearized. In the present case we have used all the occupied states and all those empty states which lie in the range 0.5 Ry from E_F. So, all the possible band-to-band transitions in the range of 0.4 Ry are properly included. Figure 4 shows $\epsilon_2(\omega)$ vs ω. In this figure there are two important peaks at about 0.11 (A) and 0.16 (B) Ry. They are due to the transitions from nonadjacent high-density peaks [Fig. 2(a)] just below the Fermi level to the first high-density region above E_F. There is a very broad peak (C) at about 0.36 Ry. In the low-energy range there is a very intense absorption at $\sim$0.04 Ry (D) and also a significant peak at $\sim$0.02 Ry (F). This last peak (F) will perhaps not be observed due to high free-electron contribution at low energies. So it will be excluded from any further discussion. Between peaks B and C there is a broad dip (E) centered at $\sim$0.29 Ry. Besides the four main peaks there are a number of other structures which will most probably be smoothed due to the relaxation τ. Unfortunately, there is no absorption-experiment data in the optical range, but the four peaks that we have mentioned above will certainly find their way in future experimental observation.

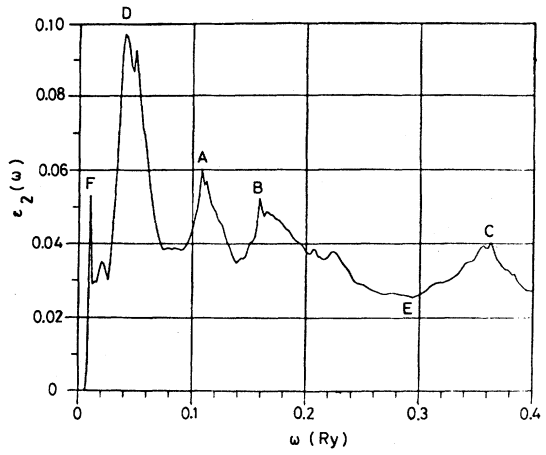

FIG. 4. Imaginary part $\epsilon_2(\omega)$ of the optical dielectric function vs energy ω (in Ry).

$\epsilon_2(\omega)$ has been also calculated by Eibler and Neck-

el.[9] They have calculated the SC BS by the APW method, but they had to interpolate this BS in the H-NFE-TB scheme to obtain the wave functions for computation of $\epsilon_2(\omega)$. They do not obtain the absorption peaks as pronounced as we do, but they do have some structures at about 1.4, 2.1, and 4.7 eV, which roughly correspond to the 0.11-, 0.16-, and 0.36-Ry peaks in our case. They also obtain a broad dip at 3.5 eV as we do at 0.29 Ry. So the overall agreement is excellent.

IV. CONCLUSION

A SC BS for FeAl is obtained by the LMTO method in the ASA. The outcome of this SC BS is used to calculate the density of states, Fermi surface, positron localization, and the imaginary part of the dielectric constant. Agreement of the density of states at the Fermi level with other theoretical calculations is found to be excellent. Experimentally, there is only one source of available data[20] and in comparison our value appears to be rather big. It is possible that the FeAl sample under study contained, perhaps, some vacancies which lowered the measured specific heat. Our $\epsilon_2(\omega)$ curve compares very well with those of Ref. 9, but we obtain many small structures besides the four main peaks. As for the Fermi surface it is the first time that it has been calculated in four principal symmetry planes. A previous calculation,[11] in the $k_z=0$ plane, does predict, as does the present work, the presence of the hole pockets at Γ. We have also calculated the Fermi surface when the Fermi level is raised by 9 mRy which eliminates the Γ hole pockets. The validity of the Fermi-surface intersection as presented here has to be confirmed by experimental studies. We hope this will be done in the near future.

ACKNOWLEDGMENTS

We wish to thank Professor E. Daniel for his constant interest in this work and for a critical reading of the manuscript.

[1]P. Ziesche, H. Wonn, Ch. Müller, V. V. Nemoshkalenko, and V. P. Krivitskii, Phys. Status Solidi B 87, 129 (1978).

[2]W. Blau, J. Weissbach, G. Merz, and K. H. Kleinstück, Phys. Status Solidi B 93, 713 (1979).

[3]Q. S. Kapoor, L. M. Watson, and D. J. Fabian, in *Band Structure Spectroscopy of Metals and Alloys,* edited by D. J. Fabian and L. M. Watson (Academic, London, 1973), p. 215.

[4]H. J. Hagemann, W. Gudet, and C. Kunz, Solid State Commun. 15, 655 (1974).

[5]M. Meurtin and P. Lesbats, Fourth International Conference on Positron Annihilation, Helsingor, Denmark, 1976 (unpublished).

[6]M. Sob, J. Phys. F 12, 571 (1982).

[7]Ch. Müller, H. Wonn, W. Blau, P. Ziesche, and V. P. Krivitskii, Phys. Status Solidi B 95, 215 (1979).

[8]R. Podloucky and A. Neckel, Phys. Status Solidi B 95, 541 (1979).

[9]R. Eibler and A. Neckel, J. Phys. F 10, 2179 (1980).

[10]D. J. Nagel, L. L. Boyer, D. A. Papaconstantopoulos, and B. M. Klein, in *Proceedings of the International Conference on the Physics of Transition Metals, Toronto, 1977,* Vol. 39 of *The Institute of Physics Conference Series,* edited by M. J. G. Lee, J. M. Perz, and E. Fawcett (IOP, London, 1978), p. 104.

[11]K. Pechter, P. Rastl, A. Neckel, R. Eibler, and K. Schwarz, Monatsh. Chem. 112, 317 (1981).

[12]O. K. Andersen, Phys. Rev. B 12, 3060 (1975).

[13]H. L. Skriver, Phys. Rev. B 14, 5187 (1976).

[14]T. Jarlborg and G. Arbman, J. Phys. F 7, 1635 (1977).

[15]D. Glötzel, B. Segall, and O. K. Andersen, Solid State Commun. 36, 403 (1980).

[16]C. Koenig, J. Phys. F 12, 1123 (1982).

[17]J. F. Janak, Phys. Rev. B 9, 3985 (1974).

[18]L. Hedin and B. I. Lundqvist, J. Phys. C 4, 2064 (1971); L. Hedin, B. I. Lundqvist, and S. Lundqvist, Solid State Commun. 9, 537 (1971).

[19]G. Lehman and M. Taut, Phys. Status Solidi B 54, 469 (1972).

[20]H. Okamoto and P. A. Beck, Monatsh. Chem. 103, 907 (1972).

[21]R. Eibler and A. Neckel, J. Phys. F 11, 1159 (1980).

[22]J. Callaway and C. S. Wang, Phys. Rev. B 16, 2095 (1977). R. A. Tawil and J. Callaway, Phys. Rev. B 7, 4242 (1973).

[23]L. Pauling, *The Nature of Chemical Bonds* (Cornell University Press, Ithaca, New York, 1960), p. 93.

[24]S. Koike, M. Hasegawa, M. Hirabayashi, and T. Suzuki, J. Phys. Soc. Jpn. 46, 1185 (1979); M. Hasegawa, M. Hirabayashi, and S. Koike, in *Proceedings of the Fifth International Conference on Positron Annihilation, Lake Yamanaka, Japan, 1979,* edited by R. R. Hasiguti and K. Fujiwara (The Japan Institute of Metals, Sendai, Japan, 1979).

[25]C. Koenig, Phys. Status Solidi B 88, 569 (1978).

[26]B. E. A. Gordon, W. E. Temmerman, and B. L. Gyorffy, J. Phys. C 11, 821 (1981).

[27]C. Y. Fong, J. Phys. F 4, 775 (1974).

[28]W. Y. Ching and J. Callaway, Phys. Rev. B 11, 1324 (1975).

[29]M. A. Khan and R. Riedinger, J. Phys. (Paris) 43, 323 (1982).

[30]A. R. Edmonds, *Angular Momentum in Quantum Mechanics* (Princeton University Press, Princeton, N.J., 1974), p. 79.